Planar Cell Polarity Protein Localization in the Secretory Ameloblasts of rat Incisors

Sumio Nishikawa and Tadafumi Kawamoto

J Histochem Cytochem published online 29 February 2012
DOI: 10.1369/0022155412438887

Planar Cell Polarity Protein Localization in the Secretory Ameloblasts of Rat Incisors

Sumio Nishikawa and Tadafumi Kawamoto

Department of Biology (SN), Radioisotope Research Institute (TK), Tsurumi University School of Dental Medicine, Yokohama, Japan

10.1369/0022155412438887

Address for correspondence:

Sumio Nishikawa

Department of Biology, Tsurumi University School of Dental Medicine

2-1-3 Tsurumi, Tsurumi-ku, Yokohama 230-8501, Japan

phone: +81-45-580-8466

FAX: +81-45-573-9599

e-mail: nishikawa-s@tsurumi-u.ac.jp

Abstract

The localization of the planar cell polarity proteins Vangl2, frizzled-3, Vangl1 and Celsr1 in the rat incisors was examined using immunocytochemistry. The results showed that Vangl2 was localized at two regions of the Tomes' processes of inner enamel-secretory ameloblasts in rat incisors: a proximal and a distal region. In contrast, frizzled-3 was localized at adherens junctions of the proximal and distal areas of inner enamel- and outer enamel-secretory ameloblasts, where N-cadherin and β-catenin were localized. frizzled-3 was also localized in differentiating inner enamel epithelial cells. Vangl1 was localized sparsely in differentiating preameloblasts and extensively at the cell boundary of stratum intermedium. Celsr1 was not localized in ameloblasts but localized in odontoblasts extensively. These results suggest the involvement of planar cell polarity proteins in odontogenesis.

Key words: ameloblasts, Vangl2, frizzled-3, Vangl1, Celsr1, planar cell polarity, immunofluorescence, enamel, rat incisor

Introduction

Epithelial cells are known to be polarized along the apical-basal axis. In addition to this apical-basal polarity, most epithelial cells have another polarity which is referred to as planar cell polarity (PCP). PCP genes and their expression have been extensively studied using *Drosophila* wings and eyes (Klein and Mlodzik, 2005; Wu and Mlodzik, 2009). *Drosophila* wing cells are polarized along the distal-proximal axis and *Drosophila* eye cells are polarized along the dorsal-ventral axis. PCP proteins are located in the noncanonical Wnt signaling pathway (van Amerogen and Berns, 2006; Klein and Mlodzik, 2005). The core PCP genes are; *frizzled*, *disheveled*, *Van Gogh* (*Vang*) (also known as *strabismus*), *prickle*, *diego* and *flamingo*. *Disheveled* is also shown to have a role in canonical Wnt/β-catenin pathway. These core PCP genes are present in all organisms from *Drosophila* to mammals, and are therefore evolutionarily conserved (Fanto and McNeill, 2004; Klein and Mlodzik, 2005; van Amerogen and Berns, 2006; Lawrence et al., 2007; Seifert and Mlodzik, 2007; Wang and Nathans, 2007; Vlader et al., 2009; Wu and Mlodzik, 2009; McNeill, 2010; Skoglund and Keller, 2010; Wallingford, 2010; Goodrich and Strutt, 2011; Wallingford and Mitchell, 2011; Wansleeben and Meijlink, 2011). The presence of *Vangl2* and *frizzled-3*, which are vertebrate genes

of *Vang* and *frizzled*, has been previously detected in dental tissue by using in situ hybridization and microarray gene expression analysis (Tissir and Goffinet, 2006). However, incisor which has been long studied because of examination of whole amelogenesis in a tooth, has not been examined. And no information of protein distribution of PCP in dental tissues is available.

PCP proteins are also involved in convergent extension of spinal cord epithelia and notochordal and somatic tissues in *Xenopus* and zebrafish (Torban et al., 2004; Keller, 2002; Keller et al., 2000; Wallingford et al., 2002; Seifert and Mlodzik, 2007). In these notochord or somite elongation processes, cells with lamellipodia at their medial or lateral end, where the actin cytoskeleton is abundant, are intercalated by pulling each other medially or laterally.

An enamel rod is a basic unit of enamel structure. The course along which an enamel rod runs varies between different regions of enamel and also between different animal teeth, including human teeth (Kawai,1955; Boyde, 1971; Osborn, 1968a,b). As expected, the movement of secretory ameloblasts during enamel secretion dictates enamel rod arrangement and orientation (Nishikawa, 1992, Hanaizumi et al., 2010). Actin and actin-related cytoskeletal components such as myosin and tropomyosin are abundant at ameloblast junctions (Nishikawa and

Kitamura, 1985a; 1986; Nishikawa et al., 1988; Nishikawa, 1992). The localization of adherens junction proteins such as N-cadherin (A-CAM), E-cadherin, β-catenin, and p120-catenin at these ameloblast junctions was previously examined (Nishikawa et al., 1990; Obara et al., 1998; Sorkin et al., 2000; Bartlett et al., 2010). However, *directional movement* of ameloblasts may require ameloblast planar cell polarization as well as a distinct localization of actin-based filament bundles. In fact, polarized distribution of actin filament bundles has been reported (Nishikawa and Kitamura, 1985b; 1986; Nishikawa et al., 1988). Since the downstream signaling pathway of planar cell polarity involves actin cytoskeleton organization, it was therefore of interest to examine the localization of PCP proteins in ameloblasts to determine if they play a role in odontogenesis.

Materials and Methods

Seventeen male Jcl Wistar rats (4-5 weeks old, 73-145 g, obtained from Clea Japan, Tokyo, Japan) were used for the present study. Institutional guidelines for animal care were followed for all experimental procedures. The animals were sacrificed by decapitation under deep anesthesia. The maxillae and mandibles were dissected and were then fixed with 4% paraformaldehyde at 4 °C overnight. Subsequently, the maxillae and mandibles were demineralized for 3 weeks at 4 °C with 5% EDTA, pH 7.2 (adjusted with concentrated NaOH solution). After washing with PBS and infusing with a 25% sucrose solution in PBS, the tissues were rapidly frozen and cryosections were made using a cryotome (HM505E, Microm, Walldorf, Germany).

Cryosections were labeled with rabbit polyclonal antibodies against a synthetic peptide corresponding to the N-terminal extracellular domain of human frizzled-3 (FZD3, LS-A4434, MBL International, Woburn, MA, USA) and goat polyclonal antibodies against a synthetic peptide corresponding to a region within the N-terminal domain of Vangl2 (N-13)(sc-46561, Santa Cruz, Santa Cruz, CA, USA). Cryosections were incubated with anti-frizzled-3 Ab diluted 1:10 with 1% bovine serum albumin in PBS (BSA-PBS) at RT for 30 min, followed by labeling with Alexa

488-conjugated donkey anti-rabbit IgG or Alexa 555-conjugated donkey anti-rabbit IgG (Invitrogen, Carmarillo, CA, USA) diluted 1:100 at RT for 30 min. Sections as negative control for stainings were incubated with normal rabbit immunoglobulin (Dako, Glostrup, Denmark) instead of the primary antibody, using an equivalent dilution, and were processed in the same way as described above. Some cryosections were labeled with anti-Vangl2 Ab at a concentration of 20 μg/ml diluted with 1% BSA-PBS, at 4 °C overnight, followed by labeling with FITC-conjugated anti-goat IgG (Santa Cruz) diluted 1:20 with 1% BSA-PBS at RT for 30 min. For staining control on sections, the anti-Vangl2 antibody solution was first incubated with excess blocking peptide (sc-46561P, Santa Cruz) for 2 hr, according to the manufacturer's instructions. Sections as negative control for stainings were then incubated with the resulting antibody-absorbed solution and processed in the same way as described above. Some other sections were labeled with anti-Vangl2 antibody, followed by ImmunoCruz Staining System (goat LSAB, Santa Cruz, sc-2053) and developed by diaminobenzidine (DAB) as chromogen.

Other cryosections were labeled with antibodies against adherens junction proteins: rabbit monoclonal anti-N-cadherin antibody (C-terminus clone EPR1792Y, Millipore, Temecula, CA, USA) and rabbit polyclonal anti-β-catenin antibody

(Millipore). Sections were labeled with anti-N-cadherin and anti-β-catenin Abs, diluted 1:50 or 1:100 with 1% BSA-PBS, at 4 °C for 30 min followed by labeling with Alexa 488-conjugated anti-rabbit IgG (Invitrogen).

For F-actin detection, sections were labeled with rhodamine-phalloidin (Invitrogen), diluted 1:50, at RT for 30 min. Cell nuclei were labeled by incubation of sections with 1 μg/ml Hoechst 33342 (Invitrogen) at RT for 30 min.

Some of the animals (nine day-old Jcl Wistar rats, Japan Clea, Tokyo, Japan) were sacrificed under deep anesthesia and rapidly frozen and freeze-dried sections were obtained without fixation and demineralization according to the method of Kawamoto (Kawamoto, 2003). Freeze-dried sections (5-μm thick) of mandibles including incisors were labeled with anti-frizzled-3 antibodies followed by Alexa 488-conjugated anti-rabbit IgG in the manner described above. Freeze-dried sections were also labeled with anti-Vangl1 (G-17, sc-46557, Santa Cruz) or anti-Celsr1 (M-125, sc-99198, Santa Cruz) diluted 1:20, followed by labeling with FITC-conjugated anti-goat IgG (Santa Cruz) or Alexa 488-conjugated anti-rabbit IgG (Invitrogen), respectively. Some sections were also labeled with Alexa Fluor 647 phalloidin (Invitrogen) diluted 1:50 for F-actin detection. Sections as negative control for stainings were incubated with 1% BSA-PBS alone for anti-Vangl1

antibody and normal rabbit IgG in 1% BSA-PBS for anti-Celsr1 antibody, resulting in no specific labelings in the dental tissues of incisors.

Fluorescent images were acquired using an Olympus AX80 fluorescence microscope equipped with a CCD camera (Quantix KAF1401E, Photometrics, Tucson, AR, USA) and using MetaMorph software (Universal imaging, Downington, PA, USA).

Results

Adherens junction protein localization in ameloblasts.

Since downstream effector of noncanonical pathway of Wnt signaling is actin cytoskeleton, actin-associated adherens junction proteins were examined. Adherens junctions of secretory ameloblasts were localized by staining for the junction markers β-catenin and N-cadherin. An N-cadherin signal was detected at the proximal and distal end of inner enamel-secretory and outer enamel-secretory ameloblasts (Fig. 1A-C). Inner enamel-secretory and outer enamel-secretory ameloblasts were classified by the shape of distal junction of each cell and arrangement of Tomes' processes of cells: the former had rectangular junction and herring bone pattern of Tomes' processes, the latter had flattened hexagonal junction and uniformly running pattern of Tomes' processes (Nishikawa et al., 1988). Based on this labeling pattern, the labeled structures were considered to be adherens junctions that are located at proximal and distal junctional complexes (Nishikawa et al., 1990; Bartlet et al., 2010). Another adherens junction protein, β-catenin, was localized at the proximal and distal junctions of inner enamel-secretory, outer enamel-secretory and early maturation ameloblasts (Figs. 1D-G and 2B,C).

Localization of frizzled-3, Vangl2 and Vangl1 in incisor enamel organ.

The localization of two PCP proteins, Vangl2 and frizzled-3, in rat incisor sections was then analyzed by immunofluorescence (Figs. 2-4). The anti-frizzled-3 Ab labeled proximal and distal junctional complexes in inner enamel-secretory ameloblasts (Figs. 2H, I, 3A, C and 4), whereas the anti-Vangl2 Ab labeled only secretory ameloblasts. The localization of frizzled-3 in freeze-dried specimens that were not fixed or demineralized was then analyzed, and frizzled-3 localization at different stages of ameloblast differentiation and enamel secretion was determined. An anti-frizzled-3 Ab signal was localized at the proximal junctional area of differentiating inner enamel epithelial cells (Fig. 4A,B). At a later stage of differentiation it became localized at the distal junctional area in addition to the proximal junctional area (Fig. 4C). In secretory ameloblasts, the anti-frizzled-3 Ab clearly labeled both the proximal and distal junctional areas (Fig. 4D-F), whereas it did not label ameloblasts at the transition zone or at maturation (Fig. 4G,H). Sections as negative control for stainings showed no specific labeling (Fig. 4I). The anti-Vangl2 antibodies strongly labeled Tomes' processes of inner enamel-secretory ameloblasts, displaying a linear staining pattern, but only weakly labeled outer enamel-secretory ameloblasts (Figs. 2A, D, G and 3B, D, F, G).

Double labeling of ameloblasts with anti-Vangl2 and anti-β-catenin Abs indicated that these proteins were localized in different regions of ameloblasts. When incisors were longitudinally sectioned, the anti-Vangl2 Ab signal was localized 6-8 μm below the anti-β-catenin-positive signal. This anti-β-catenin-positive signal was detected as a distal dotted line, and indicated adherens junctions at the distal end of the cell body (Fig. 2B, C). The anti-Vangl2 reactive signal appeared as a horizontally extended fluorescent line (Fig. 2A, C). Vertical fluorescent lines extended downwards from the horizontal linear fluorescence, towards the dentino-enamel junction, and reached up to 15 μm in height (Fig. 2A, C). Longitudinal sections were also double labeled with anti-Vangl2 and rhodamine-phalloidin (Rh-Ph), which stains F-actin at the adherens junction and at the Tomes' processes of the ameloblasts. This staining indicated a horizontal fluorescent anti-vangl2 signal at the proximal region of Tomes' processes that was similar in appearance to the staining at the distal region. This anti-Vangl2 signal was located 6 μm below the Rh-Ph-labeled distal junctional area, which appeared as a dotted line (Fig. 2D-F). Furthermore, vertical fluorescent lines were again detected with the anti-Vangl2 Ab. These lines were inclined in the apical direction of the incisor, were always attached to Rh-Ph-positive Tomes' processes (Fig. 2E, F).

Double labeling of ameloblasts with anti-Vangl2 and anti-frizzled-3 antibodies confirmed that these antibodies labeled different parts of the ameloblasts; the anti-Vangl2 Ab labeled Tomes' processes as vertical and horizontal fluorescent lines, and the anti-frizzled-3 Ab labeled the distal junctional complexes as dotted lines (Fig. 2G-I). Tangential sections of the incisor were also examined by double labeling with anti-frizzled-3 and anti-Vangl2 Abs. These sections provided profiles of transverse sections of ameloblasts, which allowed analysis of inner enamel-secretory ameloblasts. The antibody signals were clearly detected at different locations in these sections: the anti-frizzled-3 Ab signal was localized at the distal junctional complexes in the form of rectangular outlines and the anti-Vangl2 Ab signal was localized at Tomes' processes (Fig. 3A-C). In regions of the section in which enamel secretion was being initiated, an anti-Vangl2 antibody signal that had the appearance of a brown deposit was localized at the periphery of newly formed Tomes' processes (Fig. 3D). Staining control on sections that were incubated with antibody that had been pre-absorbed with excess antigen showed no specific reactivity (Fig. 3E). Double labeling with anti-Vangl2 and Rh-Ph showed that, in the middle region of the area of inner enamel secretion, anti-vangl2 was localized both around the middle part, and at the end of the distal part of Tomes'

processes that were labeled with Rh-Ph (Fig. 3F). On the other hand, little anti-Vangl2 signal could be detected at Tomes' processes in the outer enamel-secretory ameloblasts (Fig. 3G). As another *Vang* gene of vertebrates, *Vangl1* is known (Wu and Mlodzik, 2008). Anti-Vangl1 localization was, therefore, examined to know whether or not Vangl1 and Vangl2 play a redundant role in odontogenesis, using the freeze-dried specimens which were not fixed or demineralized. Anti Vangl1 Ab was localized in the stratum intermedium from differentiating enamel epithelia to papillary layer of enamel maturation zone in the incisors (Fig. 5A-D). In close examination, boundary of stratum intermedium cells was labeled as bright fluorescent dots (Fig5B, D). Inner enamel epithelial cells in the differentiating zone were also labeled as sparsely fluorescent dots (Fig. 5A, B).

Immunofluorescent localization of Celsr1 in dental tissues of the incisors.

As Celsr1 and Vangl2 are known to be necessary for orienting hair follicles and to be interdependent for their polarized hair follicle distribution (Devenport and Fuchs, 2008), Celsr1 localization was examined using the freeze-dried, unfixed and non-demineralized specimens. Anti-Celsr1-derived fluorescence was brightly localized in the cell bodies of odontoblasts but not in the ameloblasts (Fig. 5E-H).

Discussion

The presence of *Vangl2* and *frizzled-3* in dental tissue has been previously detected by using in situ hybridization and microarray gene expression analysis. Tissir and Goffinet (2006) reported strong expression of *frizzled-3* and *Vangl2* by using oligonucleotide probes in an in situ hybridization study of mouse molar tooth germ. Pemberton et al. (2007) reported that the developing mouse molar tooth showed increased expression of *Vangl2* along with increased *frizzled-6* expression, compared with control tissues. Thus, the mRNA expression of PCP genes including *Vangl2*, *frizzled-3* and *frizzled-6* in tooth germ has been shown. In the present study, the localization of Vangl2 and frizzled-3 protein was examined in rat incisor ameloblasts by immunohistochemistry. The results showed that an anti-Vangl2 Ab signal was localized at Tomes' processes of secretory ameloblasts but not in presecretory or maturation ameloblasts. In contrast, an anti-frizzled-3 Ab signal was localized at both presecretory and secretory ameloblasts, but not at maturation ameloblasts. The localization of the anti-frizzled-3 Ab signal at presecretory and secretory ameloblasts was similar to the localization previously reported for F-actin (Nishikawa et al., 1986). F-actin first appears at the proximal junctional area of differentiating ameloblasts and later appears at the distal junctional area of differentiating ameloblasts (Nishikawa and Kitamura, 1986). In secretory

ameloblasts, F-actin is continuously localized both at the proximal and distal junctional areas (Nishikawa and Kitamura, 1986). The anti-frizzled-3 Ab showed a similar localization pattern in the present study. Furthermore, F-actin filament bundles are components of adherens junctions. N-cadherin and β-catenin, which are adherens junction proteins, have been previously shown to be localized in ameloblasts (Nishikawa et al., 1990; Bartlet et al., 2010). In the present study, frizzled-3 is localized both at proximal and distal junctions, which are stained positive by antibodies of adherens junction proteins, anti-N-cadherin and anti-β-catenin.

Vangl2 and actin filament bundles are abundant in Tomes' processes of secretory ameloblasts but the frizzled-3 protein has not been localized in these processes. In the present study, Vangl2 was localized in two different regions of Tomes' processes: a proximal area and a distal area. Both of these regions appear to be associated with the secretory surface of the membrane of Tomes' processes, although ultrastructural localization of Vangl2 is necessary to clarify the stained structure. Thus, planar cell polarity (PCP) proteins appear to be involved in enamel rod formation. Vangl- and frizzled-type proteins are known to antagonize each other and to function at different cell membrane areas of the cell (Seifert and Mlodzik, 2007). PCP proteins

have been shown to play roles in tissue formation such as in alignment of mouse inner ear hair cells and *Drosophila* eyes (Seifert and Mlodzik, 2007). All PCP proteins examined in this study were localized in the incisors. As Wnt5a is known to be a representative of noncanonical Wnt pathway which is upstream signaling pathway of PCP proteins (Moon et al., 1993; Kilian et al., 2003) and *Wnt5a*-deficient mice exhibit small tooth germ (Lin et al., 2011), it is likely that PCP proteins are deeply related to tooth formation.

Mouse body hairs incline in a head-to-tail direction. The underlying molecular basis of this inclination was shown to depend on PCP proteins such as Vangl2 and the atypical cadherin Celsr1 (Devenport and Fuchs, 2008). Another member of frizzled, frizzled-6 is localized in a pattern indistinguishable from those of Vangl2 and Celsr1 in the hair follicles (Devenport and Fuchs, 2008). In incisors of rats, anti-Celsr1 was localized in different tooth-forming cells, odontoblasts. Thus, it is possible that some family proteins are associated with enamel and dentin formation to remain to be clarified. To ask the possibility of another Vang protein in the ameloblast junctions, Vangl1 was examined. Anti Vangl1 Ab was localized in the stratum intermedium. It suggests that Vangl1 may function in the formation and maintenance of cell-to-cell junction in stratum intermedium. In amelogenesis

anti-Vangl1 Ab labeled differentiating inner enamel epithelial cells as sparse bright dots, but rarely labeled in secretory ameloblasts. These distribution patterns are different from that of the frizzled-3 in this study. Thus, interaction of Vangl1 and frizzled-3 proteins is unlikely in ameloblasts. It would be interesting to know odontogenesis of knockout mice of PCP genes. Although many kind of knockout mice have been shown (van Amerongen and Berns, 2006), *looptail* and *crash* mutant mice for Vangl2 and Celsr1, respectively, are not viable after birth (Devenport and Fuchs, 2008). Knockout mice of *frizzled-3* gene are also not viable after birth (van Amerongen and Berns, 2006). Experiments of odontogenesis using these mutant mice, thus, may be limited.

In *Drosophila* wing cells, small vesicles containing frizzled are transported to adherens junctions at the cell boundary via microtubules that run in a horizontal direction (Shimada et al., 2006), suggesting that frizzled proteins are transported by microtubules that are oriented horizontally to the cell membrane. In secretory ameloblasts, most microtubules run along the long axis of the cell, that is the apical-basal axis, but some microtubules do run horizontally, i.e., along the orthogonal plane of the apical-basal axis at the level of the distal junctional complex (Nishikawa and Kitamura, 1985a). It is therefore possible that material important

for junctional membranes, including frizzled-3, may be transported by microtubules in secretory ameloblasts. Since frizzled is a Wnt receptor, and a noncanonical downstream signaling pathway of frizzled is actin cytoskeleton reorganization (van Amerongen and Berns, 2006; Klein and Mlodzik, 2005), the presence of frizzled in ameloblast junctional complexes may induce the formation of, and maintain, actin cytoskeleton structure via the regulation of a small G protein such as RhoA. The small G proteins RhoA and Rac, as well as the Rho kinase Rock, are known downstream components of frizzled receptor signaling (van Amerongen and Berns, 2006; Klein and Mlodzik, 2005). Inhibition of Rho kinase was reported to mimic PCP-linked defects (Yates et al., 2010). Furthermore, Rho GTPases such as RhoA and Rac, as well as their regulator molecules, have been shown to function in amelogenesis (Li et al., 2005; Hatakeyama et al., 2009; Biz et al., 2010; Ohtsu et al., 2010; Li et al., 2011).

Although the characteristic localization of frizzled-3 and Vangl2 in ameloblasts strongly suggests the involvement of PCP proteins in tooth enamel formation, further studies are obviously needed, to confirm their involvement and to understand their mechanism of action.

References

Bartlett JD, Dobeck JM, Tye CE, Perez-Moreno M, Stokes N, Reynolds AB, Fuchs E, Skobe Z. 2010. Targeted p120-catenin ablation disrupts dental enamel development. PLoS ONE 5(9): e12703. doi:10.1371/journal.pone.0012703.

Biz MT, Marques MR, Crema VA, Moriscot AS, dos Santos MF. 2010. GTPases RhoA and Rac1 are important for amelogenin and DSPP expression during differentiation of ameloblasts and odontoblasts. Cell Tissue Res 340:459-470.

Boyde A. 1971. Comparative histology of mammalian teeth. In: Dental morphology and evolution, AA Dahlberg, ed. University of Chicago Press. Chicago. p.81-94.

Devenport D, Fuchs E. 2008. Planar polarization in embryonic epidermis orchestrates global asymmetric morphogenesis of hair follicles. Nat Cell Biol. 11:1257-1268.

Fanto M, McNeill H. 2004. Planar polarity from flies to vertebrates. J Cell Sci 117:527-533.

Goodrich LV, Strutt D. 2011. Principles of planar polarity in animal development. Development 138:1877-1892.

Hanaizumi Y, Yokota R, Domon T, Wakita M, Kozawa Y. 2010. The initial process of enamel prism arrangement and its relation to the Hunter-Schreger bands in dog teeth. Arch Histol Cytol 73:23-36.

Hatakeyama J, Fukumoto S, Nakamura T, Haruyama N, Suzuki S, Hatakeyama Y, Shum L, Gibson CW, Yamada Y, Kulkarni AB. 2009. Synergistic roles of amelogenin and ameloblastin. J Dent Res 88:318-322.

Kawai N. 1955. Comparative anatomy of the bands of Schreger. Okajimas Folia Anat Jpn. 27:115-131.

Kawamoto T. 2003 Use of a new adhesive film for the preparation of multi-purpose fresh-frozen sections from hard tissues, whole-animals, insects and plants. Arch Histol Cytol. 66:123-143

Keller R. 2002. Shaping the vertebrate body plan by polarized embryonic cell movements. Science. 298:1950-1954.

Keller R, Davidson L, Edlund A, Elul T, Ezin M, Shook D, Skoglund P. 2000. Mechanisms of convergence and extension by cell intercalation. Phil Trans R Soc Lond B. 355:897-922.

Kilian B, Mansukoski H, Barbosa FC, Ulrich F, Tada M, Heisenberg CP. 2003. The role of Ppt/Wnt5a in regulating cell shape and movement during zebrafish gastrulation. Mech Dev 120:467-476.

Klein TJ, Mlodzik M. 2005. Planar Cell polarization: an emerging model points in the right direction. Annu Rev Cell Dev Biol. 21:155-176.

Lawrence PA, Struhl G, Casal J. 2007. Planar cell polarity: one or two pathways? Nat Rev Genet 8:555-563.

Li Y, Decker S, Yuan Z, DenBesten PK, Aragon MA, Jordan-Sciutto K, Abrams WR, Huh J, McDonald C, Chen E, MacDougall M, Gibson CW. 2005. Effects of sodium fluoride on the actin cytoskeleton of murine ameloblasts. Archs Oral Biol 50:681-688.

Li Y, Pugach MK, Kuehl MA, Peng L, Bouchard J, Hwang SY, Gibson CW. 2011. Dental enamel structure is altered by expression of dominant negative RhoA in ameloblasts. Cells Tissues Organs 194:2-4

Lin M, Li L, Liu C, Liu H, He F, Yan F, Zhang Y, Chen Y. 2011. Wnt5a regulates growth, patterning, and odontoblast differentiation of developing mouse tooth. Dev Dyn 240:432-440.

McNeill H. 2010. Planar cell polarity: keeping hairs straight is not so simple. Cold Spring Harb Perspect Biol 2:a003376.

Moon RT, Campbell RM, Christian JL, McGrew LL, Shih J, Fraser S. 1993. *Xwnt*-5a: a maternal *Wnt* that affects morphogenetic movements after

overexpression in embryos of *Xenopus laevis*. Development 119:97-111.

Nishikawa S. 1992. Correlation of the arrangement pattern of enamel rods and secretory ameloblasts in pig and monkey teeth: a possible role of the terminal webs in ameloblast movement during secretion. Anat Rec 232:466-478.

Nishikawa S, Kitamura H. 1985a. Three-dimensional network of microtubules in secretory ameloblasts of rat incisors. Archs Oral Biol. 30:1-11.

Nishikawa S, Kitamura H. 1985b. Actin filaments in the terminal webs of secretory ameloblasts of rats. Archs Oral Biol. 30:13-21.

Nishikawa S, Kitamura H. 1986. Localization of actin during differentiation of the ameloblast, its related epithelial cells and odontoblasts in the rat incisor using NBD-phallacidin. Differentiation 30:237-243

Nishikawa S, Fujiwara K, Kitamura H. 1988. Formation of the tooth enamel rod pattern and the cytoskeletal organization in secretory ameloblasts of the rat incisor.

Eur J Cell Biol 47:222-232.

Nishikawa S, Tsukita S, Tsukita S, Sasa S. 1990. Localization of adherens junction proteins along the possible sliding interface between secretory ameloblasts of the rat incisor. Cell Struct Funct. 15:245-249.

Obara N, Suzuki Y, Nagai Y, Takeda M. 1998. Expression of E- and P-cadherin during tooth morphogenesis and cytodifferentiation of ameloblasts. Anat Embryol. 197:469-475.

Osborn JW. 1968a. Evaluation of previous assessments of prism directions in human enamel. J Dent Res. 47:217-222.

Osborn JW. 1968b. Directions and interrelationships of enamel prisms from the sides of human teeth. J Dent Res 47:223-232.

Otsu K, Kishigami R, Fujiwara N, Ishizeki K, Harada H. 2010. Functional role of Rho-kinase in ameloblast differentiation. J Cell Physiol 226:2527-2534.

Pemberton TJ, Li F-Y, Oka S, Mendoza-Fandino GA, Hsu Y-H, Bringas, Jr P, Chai Y, Snead ML, Mehrian-Shai R, Patell PI. 2007. Identification of novel genes expressed during mouse tooth development by microarray gene expression analysis. Dev Dyn 236:2245-2257.

Seifert JRK, Mlodzik M. 2007. Frizzled/PCP signaling: a conserved mechanism regulating cell polarity and directed motility. Nat Rev Genet. 8:126-138.

Shimada Y, Yonemura S, Ohkura H, Strutt D, Uemura T. 2006. Polarized transport of Frizzled along the planar microtubule arrays in *Drosophila* wing epithelium. Dev Cell. 10:209-222.

Skoglund P, Keller R. 2010. Integration of planar cell polarity and ECM signaling in elongation of the vertebrate body plan. Curr Opin Cell Biol 22:589-596.

Sorkin BC, Wang MY, Dobeck JM, Albergo KL, Skobe Z. 2000. The cadherin-catenin complex is expressed alternately with the adenomatous polyposis coli protein

during rat incisor amelogenesis. J Histochem Cytochem. 48:397-406.

Tissir F, Goffine AM. 2006. Expression of planar cell polarity genes during development of the mouse CNS. Eur J Neurosci. 25:597-607.

Torban E, Kor C, Gros P. 2004. Van Gogh-like2 (Strabismus) and its role in planar cell polarity and convergent extension in vertebrates. Trends Genet. 20:570-577.

van Amerongen R, Berns A. 2006. Knockout mouse models to study Wnt signal transduction. Trends Genet. 22:678-689.

Vladar EK, Antic D, Axelrod JD. 2009. Planar cell polarity signaling: the developing cell's compass. Cold Spring Harb Perspect Biol 1:a002964.

Wallingford JB. 2010. Planar cell polarity signaling, cilia and polarized ciliary beating. Curr Opin Cell Biol 22:597-604.

Wallingford JB, Mitchell B. 2011. Strange as it may seem: the many links between

Wnt signaling, planar cell polarity, and cilia. Genes Dev 25:201-213.

Wallingford JB, Fraser SE, Harland RM. 2002. Convergent extension: the molecular control of polarized cell movement during embryonic development. Dev Cell. 2:695-706.

Wang Y, Nathans J. 2007. Tissue/planar cell polarity in vertebrates: new insights and new questions. Development 134:647-658

Wansleeben C, Meijlink F. 2011. The planar cell polarity pathway in vertebrate development. Dev Dyn 240:616-626.

Wu J, Mlodzik M. 2009. A quest for the mechanism regulating global planar cell polarity of tissues. Trends Cell Biol.19:295-305.

Wu J, Klein TJ, Mlodzik M. 2004. Subcellular localization of frizzled receptors, mediated by their cytoplasmic tails, regulates signaling pathway specificity PLos Biol. 2:E158.

Yates LL, Schnatwinkel C, Murdoch JN, Bogani D, Formstone CJ, Townsend S, Greenfield A, Niswander LA, Dean CH. 2010. The PCP genes *Celsr1* and *Vangl2* are required for normal lung branching morphogenesis. Hum Mol Genet. 19:2251-2267.

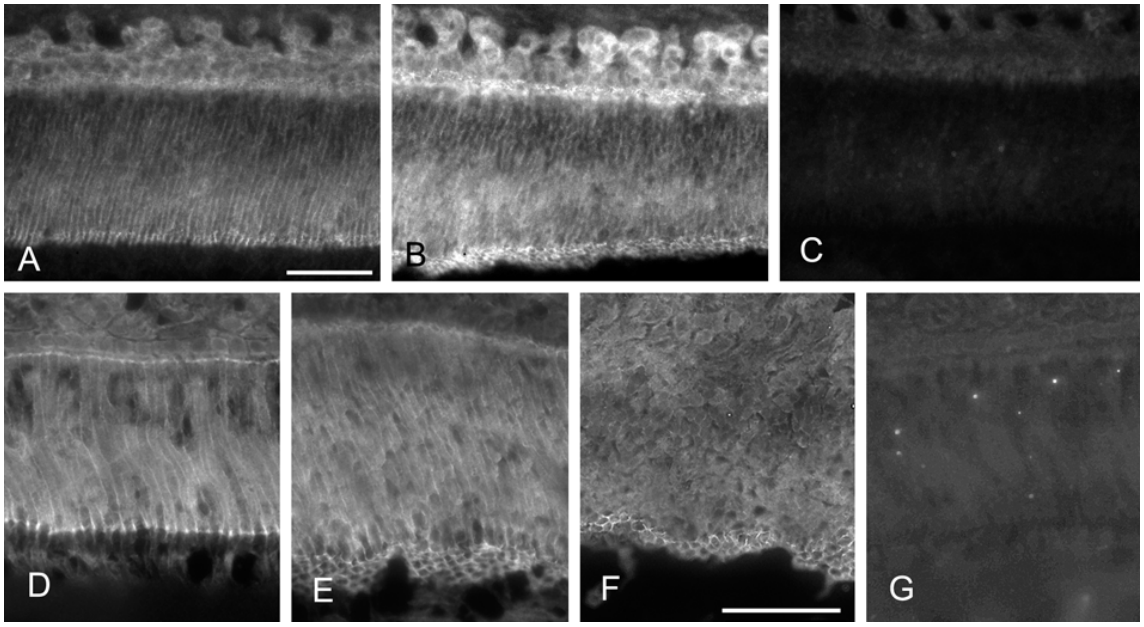

Fig. 1. Immunofluorescent localization of anti-N-cadherin and anti-β-catenin antibody signals in the ameloblasts of rat mandibular incisors. Sections of rat mandibular incisors were immunohistochemically stained with anti-N-cadherin (A, B) or anti-β-catenin (D, E, F) antibodies. Sections as negative control for anti-N-cadherin (C) and anti-β-catenin (G) are also shown. Inner enamel-secretory (A, C, D, G), outer enamel secretory- (E), outer enamel-secretory to transitional (B) and transitional (F) ameloblasts are shown. An anti-N-cadherin antibody signal was detected at the proximal and distal junctions of inner enamel- and outer enamel-secretory ameloblasts (A, B). The Sections as negative control shows no specific labeling (C). An anti-β-catenin antibody signal was also detected at the proximal and distal junctional complexes in inner enamel- and outer enamel-secretory ameloblasts as well as at the distal cell end of transitional

amelobasts (D, E, G). No specific reactivity was observed in the section as negative control (G). Bars=50 μm.

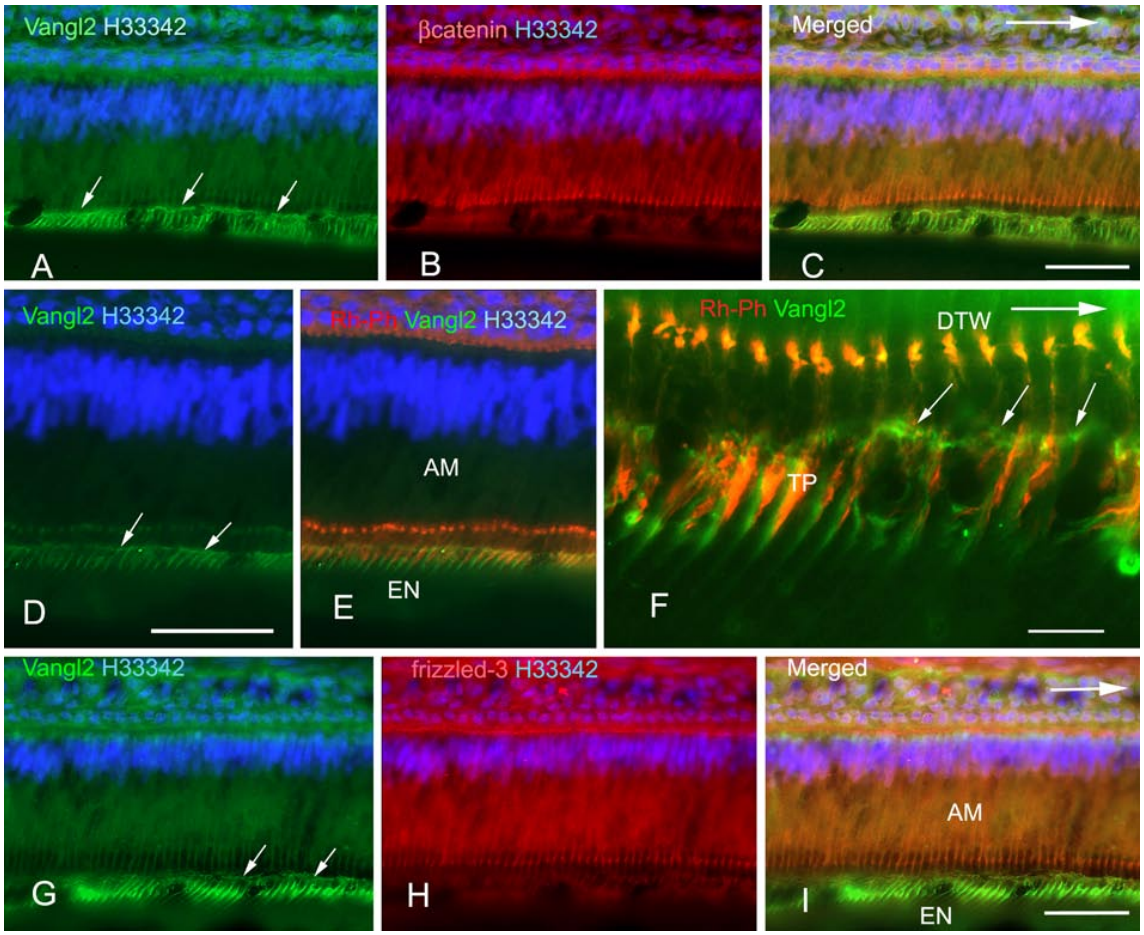

Fig. 2. Triple labeling of inner enamel-secretory ameloblasts with anti-Vangl2 and Hoechst 33342 (H33342), and either anti-β-catenin, rhodamine-phalloidin or anti-frizzled-3. Sections of rat incisors were stained with anti-Vangl2 Ab (A, C-G, I) (green), anti-β-catenin (B, C) (red), rhodamine-phalloidin (Rh-Ph) (E, F) (red), or anti-frizzled-3 (H, I) (red), and nuclei were stained with Hoechst 33342 (H33342) (A-E,G-I) (blue). A merged image of (A) and (B) is shown in (C). An anti-Vangl2 Ab-labeled horizontal fluorescent line (arrows in A, D, F, G) was localized at the

proximal part of Tomes' processes. This region was located 5-10 μm below the distal junctional complexes that were labeled with anti-β-catenin (B, C) or F-actin (E, F). Anti-frizzled-3 antibodies labeled distal junctional complexes (H, I). Anti-Vangl2-labeled vertical fluorescent lines were also seen below the horizontal fluorescent line in Tomes' processes (A, C-G, I). Double-labeling of Tomes' processes (TP in F) with anti-Vangl2 Ab and rhodamine phalloidin showed that these vertical fluorescent lines were localized at the lateral surface of Tomes' process on the apical side of the incisor (F). The arrows indicate the incisal direction. AM, ameloblast; EN, enamel; DTW, distal terminal web; TP, Tomes' process. (C, D, I) Bars=50 μm. (F) Bar=10 μm.

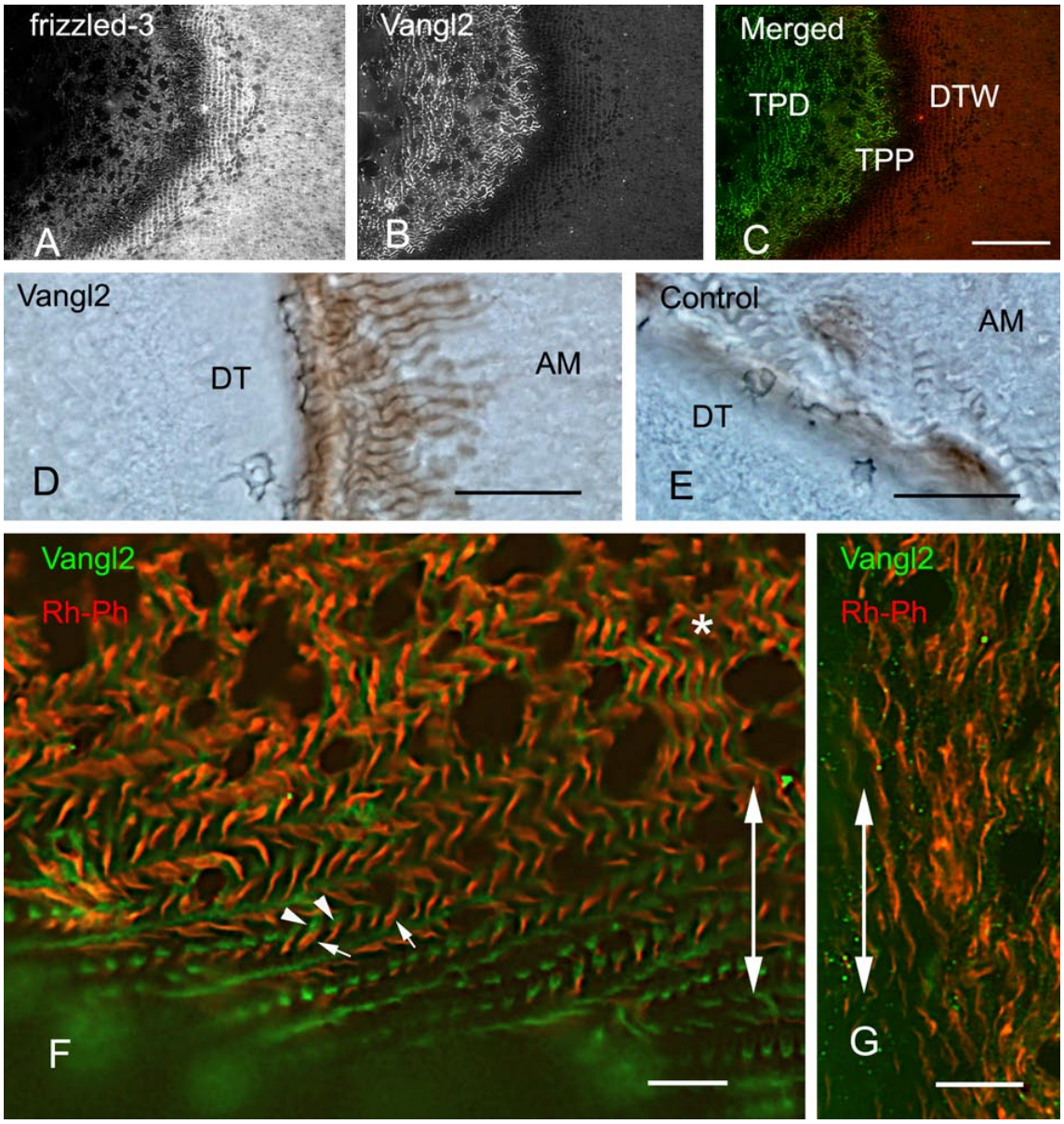

Fig. 3. Labeling of Vangl2, frizzed-3 and actin in tangential sections of ameloblasts. Tangential sections of rat incisors at the level of Tomes' processes and the distal terminal web at the zone of inner enamel secretion (A-F) and of outer enamel secretion (G) are shown. A-C: Double labeling with anti-frizzled-3 and anti-Vangl2. The anti-frizzled-3 Ab labeled distal junctional complexes (DTW) but not Tomes'

processes (A, C), whereas the anti-Vangl2 Ab labeled proximal and distal parts of Tomes' processes (TPP and TPD, respectively) but not distal junctional complexes (B, C). D, E: Anti-Vangl2 localization in early enamel formation visualized by immunoperoxidase followed by DAB staining, showed brown positive reactivity around the newly formed Tomes' processes (D). The staining control on section which was incubated with anti-Vangl2 antibodies preabsorbed with excess antigen, showed no specific reactivity (E). DT. dentin; AM, ameloblast. F, G: Double labeling with the anti-Vangl2 antibody and with rhodamine phalloidin for F-actin detection. Whole Tomes' processes were labeled with rhodamine-phalloidin (red). Distal Parts of Tomes' processes were shown by small arrows (F). In the area of inner enamel secretion (F), the anti-Vangl2 Ab (green) labels the periphery of the proximal part of Tomes' processes (F, asterisk) and also labels one side of the distal part of Tomes' processes (F, arrowheads), whereas in the area of outer enamel secretion (G), only long slender fluorescent Tomes' processes (red) and weak anti Vangl2 Ab fluorescence (green) were observed. Large double pointed arrows (F, G) show the long axis of the incisor. (C) Bar= 50 μm. (D, E) Bars= 20 μm. (F, G) Bars= 10 μm.

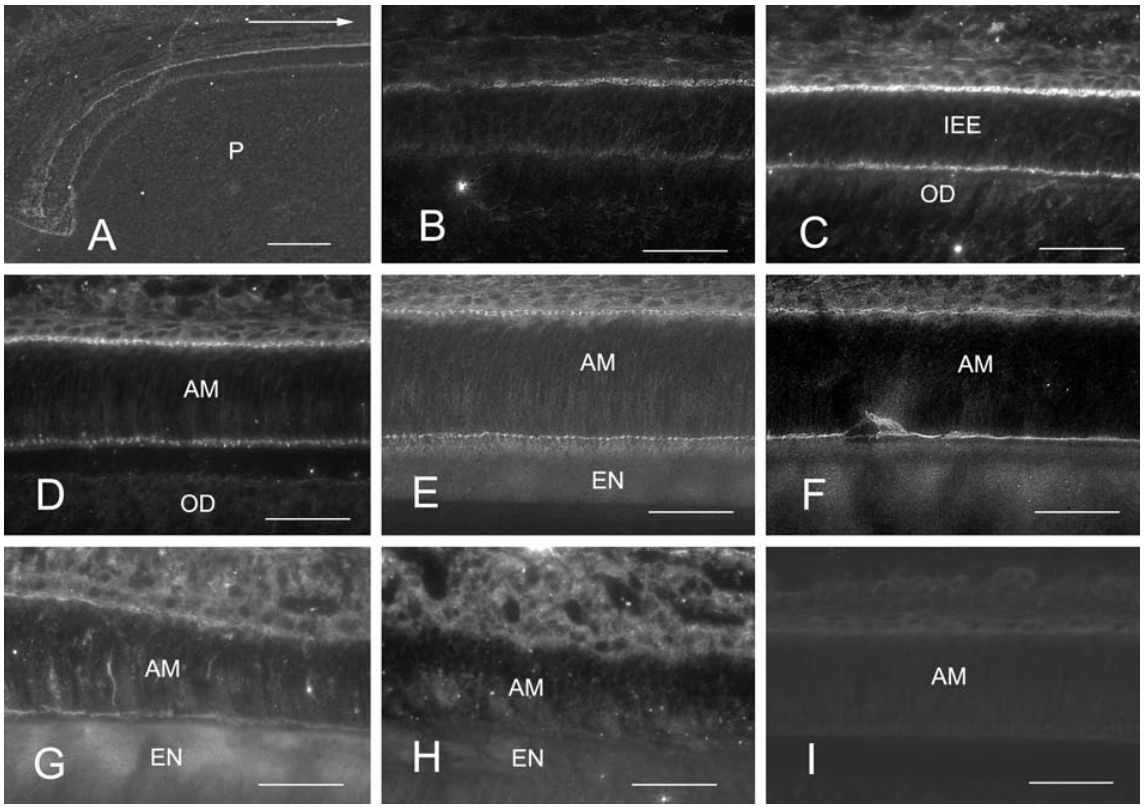

Fig.4 Frizzled-3 labeling of freeze-dried sections of rat incisors without fixation and demineralization. Anti-frizzled-3 labeling (A-H) of inner enamel epithelia and ameloblasts at the following stages are shown: proliferation (A), early differentiation (B), late differentiation (C), early inner enamel secretion (D), middle inner enamel secretion (E), outer enamel secretion (F), transition (G), and early maturation (H). A section for negative control is also shown (I). Initially, the proximal part of the inner enamel epithelia was anti frizzled-3-Ab-positive (A, B). The distal part then became positive in late differentiation (C). Both proximal and distal junctional complexes in the region of inner and outer enamel secretion were positive (D-F), but fluorescence gradually diminished at the transition zone (G), and

disappeared in the zone of maturation (H). The section for negative control showed no specific labeling (I). Odontoblasts showed no labeling with the anti-frizzled-3 Ab (C, D). The arrow in A shows incisal direction. IEE, inner enamel epithelial cell; AM, ameloblast; EN, enamel; OD, odontoblast. Bars=50 μm.

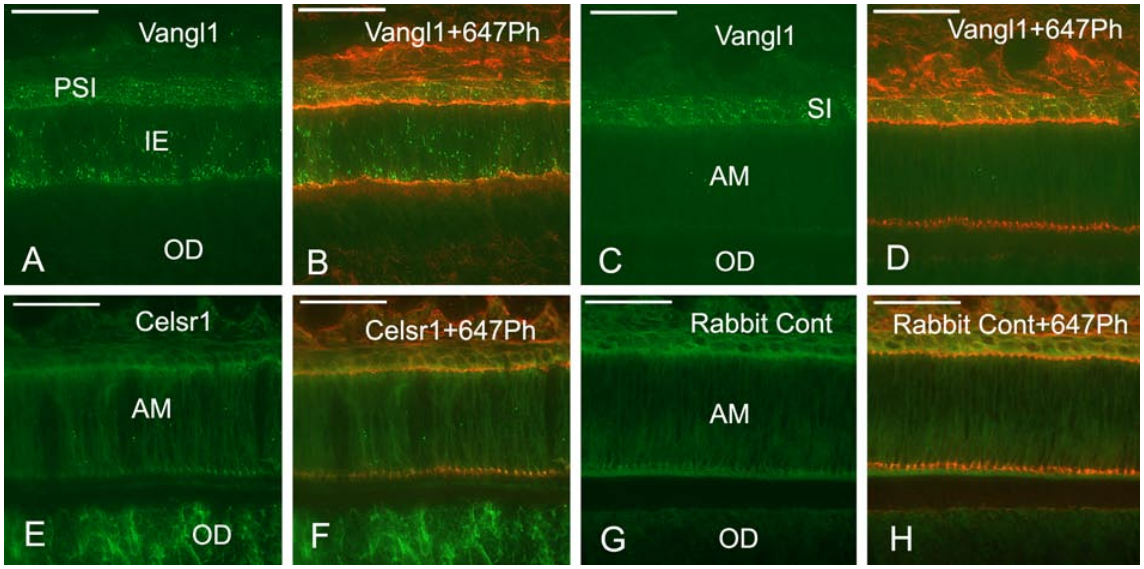

Fig.5 Vangl1 and Celsr1 labeling of freeze-dried sections of rat incisors without fixation and demineralization. Double labeling of differentiating inner epithelia (IE) and provisional stratum intermedium (PSI) (A, B) and inner enamel secretory ameloblasts (AM) and stratum intermedium (SI) (C, D) with anti-Vangl1 (A-D, green) and Alexa 647 phalloidin (B, D, red). Double labeling of inner enamel secretory ameloblasts (AM) and odontoblasts (OD) with anti-Celsr1 (E, F, green) and Alexa 647 phalloidin (F, red). Section as negative control for staining was incubated with normal rabbit IgG followed with Alexa 488-conjugated anti-rabbit IgG (G, H, green) and Alexa 647 phalloidin (H, red). Anti-Vangl1 labels differentiating preameloblasts and provisional stratum intermedium as bright fluorescent dots (A, B), and stratum intermedium but not secretory ameloblasts (C,

D). Anti-Celsr1 labels odontoblasts extensively but does not label ameloblasts (E, F), whereas the section as negative control for staining incubated with normal rabbit antibody shows no specific labeling in odontoblasts or ameloblasts (G, H). Bars=50 μm.